Interface spin waves in a bilayer of two-sublattice ferrimagnets

Hao Che and Yu Xia
Chinese Center of Advanced Science and Technology (World Laboratory), Beijing 100080, People's Republic of China and Southwestern Institute of Physics, P.O. Box 432, Chengdu, Sichuan 610041, People's Republic of China

D. L. Lin
Department of Physics and Astronomy, State University of New York at Buffalo, Buffalo, New York 14260

Xiaoming Qiu
Southwestern Institute of Physics, P.O. Box 432, Chengdu, Sichuan 610041, People's Republic of China

Hang Zheng
Chinese Center of Advanced Science and Technology (World Laboratory), Beijing 100080, People's Republic of China and Department of Applied Physics, Shanghai Jaio Tong University, Shanghai 200030, People's Republic of China

(Received 17 December 1990)

Interface spin waves (ISW) in a bilayer of two-sublattice ferrimagnets are investigated on the Heisenberg model with nearest-neighbor exchange interactions. We first derive the Green's functions for the bilayer system in different coupling schemes and express them in terms of Green's functions for the two semi-infinite ferrimagnetic systems that are already known from previous work. Interface-spin-wave spectra are then calculated from these functions for various interface-coupling schemes. When the two semi-infinite systems are different, it is found that there are two ISW's localized in the interface, one on each side, for any finite interface exchange coupling J_{12} and that they always appear outside the energy range of the corresponding surface spin waves (SSW) of the two semi-infinite ferrimagnets. Hence the SSW's serve as the lower bounds of the ISW's in the energy spectra. In the limit of $J_{12}\rightarrow 0$, the ISW's approach their corresponding SSW's as expected.

I. INTRODUCTION

A considerable amount of work on interface spin waves (ISW)[1-6] has been performed in recent years for heterostructures of magnetic materials and magnetic superlattices. In the earliest paper we can find in the literature, Yaniv[1] considered the interface between two semi-infinite simple cubic Heisenberg ferromagnets. Using the Green's-function technique, he studied the ISW on the (100) interface formed by the nearest-neighbor exchange coupling between the surface layers of the two components. It is found that there may be zero, one, or two branches of ISW's depending on the interface exchange integral and other parameters of the two materials.

Ferromagnetic interface spin waves in cubic Heisenberg systems are also discussed by Xu, Mostoller, and Rajagopal.[2] Very different results are obtained for different faces of the same crystal, or for the same face of different crystals. Magnetic superlattices of ferromagnetic and antiferromagnetic materials have been discussed by Herman, Lambia, and Jepsen,[3] Hinchey and Mills,[4] and Diep.[5] Mika and Grunberg[6] have considered a ferromagnetic multilayer with alternating directions of magnetization and a semi-infinite stack of alternating films of two different ferromagnets has been treated by Dobrzynski, Djafari-Rouhani, and Puszkarski.[7] Very recently, Mata and Pestana[8] have investigated the nature of ISW as a function of exchange coupling strengths at the interface between two antiferromagnets and found a variety of possible magnon states.

On the other hand, there have been only ferrimagnetic surface-spin-wave (SSW) treatments[9-12] in the literature, and we have not found any work on ferrimagnetic interface waves. Hung, Harada, and Nagai[9] assume the two sublattices with opposite spins forming a CsCl structure, while Zheng and Lin[11] consider a semi-infinite ferrimagnet consisting of two different kinds of magnetic ions a and b forming two sublattices with the mean spin values $|\langle S^z\rangle_a|\neq|\langle S^z\rangle_b|$. Both the CsCl and NaCl structures are treated in Ref. 11 by the method of retarded Green's-function equations of motion in the matrix form. The method used in Ref. 11 was introduced by Lin and Zheng.[12] It greatly simplifies the algebraic procedure and is particularly useful in the treatment of surface or interface spin waves in ferrimagnetic systems.

We apply the method of Ref. 12 to investigate in this article the nature of ISW's and their spectra in a bilayer heterostructure of ferrimagnets with CsCl structures. We consider two semi-infinite ferrimagnets of different spins coupled to each other via nearest-neighbor interactions between their (001) surfaces. Thus, the Green's function for a semi-infinite system derived in Ref. 11 can be em-

ployed directly as our starting point. Since the results of Ref. 11 will be frequently quoted in this paper, we refer to it as I from now on.

The plan of this paper is as follows. We first describe the model in Sec. II. Four different types of interface coupling are defined here. The interface Green's functions are derived in Sec. III from the semi-infinite Green's functions and expressed in terms of the bulk Green's function. In Sec. IV, ISW spectra of a variety of possible modes in our model are calculated, and numerical results are discussed in detail in Sec. V.

II. MODEL OF FERRIMAGNETIC INTERFACES

We consider the (001) interface between two semi-infinite Heisenberg ferrimagnets. Each is a two-sublattice system forming a CsCl structure, namely, a body-centered-cubic (bcc) lattice with the two sublattices themselves simple cubic. Figure 1 shows schematically two cases of interface contact projected on the (010) plane. In Fig. 1(a), the system as a whole maintains the bcc structure throughout. The nearest neighbors on two sides of the interface lie along the diagonal direction. The case in Fig. 1(b) can be obtained by displacing one ferrimagnet in (a) by $\frac{1}{2}$ lattice constant in both x and y directions. The nearest neighbors on two sides of the interface are then along the direction normal to the interface. The z axis is chosen to be perpendicular to the interface. The atomic layers parallel to the interface are labeled by $n=\ldots,-3,-2,-1,0,1,2,3,\ldots$ with the interface located between the layers -1 and 0. Type-1 material occupies the left space and type-2 material occupies the right space. In each material, the mean spins of the two sublattices are opposite in directions. The bilayer system can have three different types of interface: (1) an a-b antiferromagnetic interface which is formed by the a-sublattice surface of one material coupled to the b-sublattice surface of the other material via the coupling $J_{12}>0$ as in Figs. 1(a) and 1(b), (2) an a-a ferromagnetic interface which is formed by the two a-sublattice surfaces via the coupling $J_{12}<0$, and (3) a b-b ferromagnetic interface which is obtained by interchanging the a and b sublattices and hence is equivalent to the a-a ferromagnetic interface in (2).

To keep the calculation manageable, we assume as usual that the interface does not change the mean spin values in any sublattice near the interface. This means that $\langle S_a^z\rangle^{(i)}=\langle S^z\rangle_a^{(i)}$, $\langle S_b^z\rangle^{(i)}=\langle S^z\rangle_b^{(i)}$, where $i=1,2$ for the two ferrimagnets. For convenience, we also define

$$\alpha_i=-\langle S^z\rangle_b^{(i)}/\langle S^z\rangle_a^{(i)},\quad i=1,2\ . \tag{1}$$

In either semi-infinite system, the nearest neighbors of an a spin are all b spins and vice versa. The Heisenberg model Hamiltonian for the nearest-neighbor interaction can then be written as

$$H=\sum_{a,b} J\mathbf{S}_a\cdot\mathbf{S}_b\ , \tag{2}$$

where J denotes the nearest-neighbor exchange integral, and the sum is taken over the nearest-neighboring pair of spins only once. J can have only three different values, it is taken to be J_1 (J_2) when the pair belongs to material 1 (2), and J_{12} when the pair belongs to different materials across the interface. We shall make liberal use of the results of I and follow the same notation except for the superscript (i) to label the two semi-infinite systems in the present case.

III. INTERFACE GREEN'S FUNCTIONS

In this section we limit our discussion to the a-b antiferromagnetic interface coupling as in Fig. 1(a). The other cases will be discussed in Sec. IV. We first consider the special case $J_{12}=0$ in which the bilayer system is decoupled and becomes two separate semi-infinite ferrimagnets. The results of I can be directly taken up and we have, following Eq. (41) of I, for the two semi-infinite systems

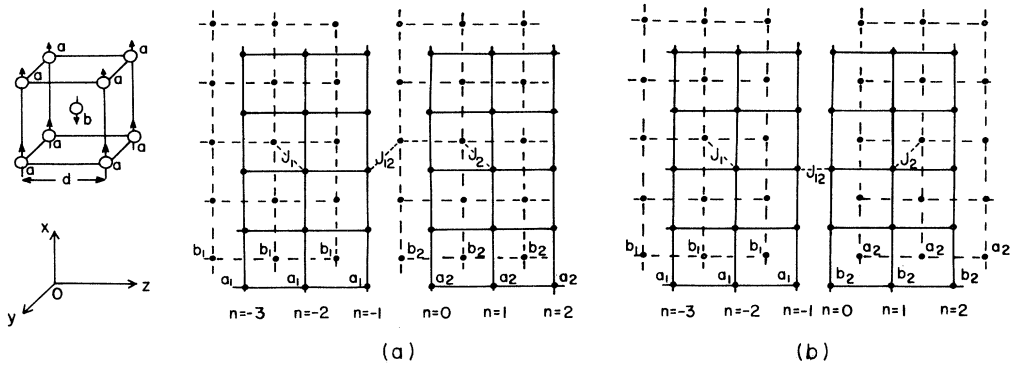

FIG. 1. Illustration of the interface structure of a bilayer of ferrimagnets with CsCl structures. The picture shows its projection on the (010) plane while the interface is parallel to (001) plane. The nearest-neighbor coupling across the interface is a-b antiferromagnetic in both (a) and (b). A unit cell and the coordinate axes are also shown at the left end.

$$\underline{G}^{(1)}(m,n)=\underline{g}^{(1)}(m,n)+[\underline{g}^{(1)}(m,-1)\underline{V}^{(1)}_{ba}+\underline{g}^{(1)}(m,0)\underline{V}^{(1)}_{1f}]\times[\underline{1}-\underline{g}^{(1)}(-1,-1)\underline{V}^{(1)}_{ba}-\underline{g}^{(1)}(-1,0)\underline{V}^{(1)}_{2f}]^{-1}\underline{g}^{(1)}(-1,n)\ , \tag{3}$$

where $m,n\le -1$ and

$$\underline{G}^{(2)}(m,n)=\underline{g}^{(2)}(m,n)+[\underline{g}^{(2)}(m,0)\underline{V}^{(2)}_{bb}+\underline{g}^{(2)}(m,-1)\underline{V}^{(2)}_{1f}]\times[\underline{1}-\underline{g}^{(2)}(0,0)\underline{V}^{(2)}_{bb}-\underline{g}^{(2)}(0,-1)\underline{V}^{(2)}_{1f}]^{-1}\underline{g}^{(2)}(0,n)\ , \tag{4}$$

where $m,n\ge 0$. $\underline{1}$ is a unit matrix and the coupling matrices are

$$\underline{V}^{(1)}_{ba}=\begin{bmatrix}4J_1\langle S^2\rangle^{(1)}_b & 0\\ 0 & 0\end{bmatrix}\ , \tag{5a}$$

$$\underline{V}^{(1)}_{2f}=\begin{bmatrix}0 & 0\\ -4J_1\langle S^z\rangle^{(1)}_b\eta(\kappa) & 0\end{bmatrix}\ , \tag{5b}$$

$$\underline{V}^{(2)}_{bb}=\begin{bmatrix}0 & 0\\ 0 & 4J_2\langle S^z\rangle^{(2)}_a\end{bmatrix}\ , \tag{6a}$$

$$\underline{V}^{(2)}_{1f}=\begin{bmatrix}0 & -4J_2\langle S^z\rangle^{(2)}_a\eta(\kappa)\\ 0 & 0\end{bmatrix}\ . \tag{6b}$$

All the Green's functions in (3) and (4) above are 2×2 matrices. They are all functions of the energy E and the two-dimensional wave vector κ defined by $\mathbf{k}=(\kappa,q)=(k_x,k_y,q)$. These variables are omitted in expressions throughout this paper only for simplicity. $g^{(i)}(m,n)$ are the bulk Green's function for the ith ferrimagnet. They are, according to Eq. (45) of I, given by

$$\underline{g}^{(i)}(m,n)=\frac{1}{8J_i\langle S^z\rangle^{(i)}_a}\frac{1}{\frac{1}{2}\alpha_i\eta^2(\kappa)}\times\begin{bmatrix}\dfrac{i(\varepsilon_i+1)}{U_i(\mathbf{k})}W^{|m-n|} & \frac{1}{2}\eta(\kappa)Z^{(i)}_{+}\\ -\frac{1}{2}\alpha_i\eta(\kappa)Z^{(i)}_{-} & \dfrac{I(\varepsilon_i-\alpha_i)}{U_i(\kappa)}W^{|m-n|}\end{bmatrix}\ . \tag{7}$$

$$Z^{(i)}_{\pm}(\kappa)=\frac{i}{U_i(\kappa)}\{[W_i(\kappa)]^{|m-n|}+[W_i(\kappa)]^{|m-n\pm 1|}\}\ , \tag{8}$$

$$U_i(\kappa)=\begin{cases}i\ \mathrm{sgn}(T_i)[T_i^2(\kappa)-1]^{1/2}, & T_i^2(\kappa)>1\ ,\\ -\mathrm{sgn}\left[\varepsilon_i-\dfrac{\alpha_i-1}{2}\right]\sqrt{1-T_i^2(\kappa)}, & T_i^2(\kappa)<1\ .\end{cases} \tag{9}$$

$$T_i(\kappa)=1+(\varepsilon_i+1)(\varepsilon_i-\alpha_i)\Big/\frac{\alpha_i}{2}\eta^2(\kappa)\ , \tag{10}$$

$$W_i(\kappa)=-T_i(\kappa)-iU_i(\kappa)\ , \tag{11}$$

$$\eta(\kappa)=\cos(k_x d)\cos(k_y d)\ , \tag{12}$$

$$\varepsilon_i=E/8J_i\langle S^Z\rangle^{(i)}_a\ , \tag{13}$$

where d represents the nearest-neighbor distance.

It has been shown in I that there is a SSW in medium 1 and its spectrum is given by

$$\varepsilon_1^{\mathrm{SSW}}(\kappa)=-\tfrac{1}{2}(1-\tfrac{1}{2}\alpha_1-\tfrac{1}{2}\eta^2)+\tfrac{1}{2}[(1-\tfrac{1}{2}\alpha_1-\tfrac{1}{2}\eta^2)^2+2\alpha_1(1-\eta^2)]^{1/2} \tag{14}$$

and the SSW spectrum in medium 2 is given by

$$\varepsilon_2^{\mathrm{SSW}}(\kappa)=-\tfrac{1}{2}(\tfrac{1}{2}-\alpha_2+\tfrac{1}{2}\alpha_2\eta^2)-\tfrac{1}{2}[(\tfrac{1}{2}-\alpha_2+\tfrac{1}{2}\alpha_2\eta^2)^2+2\alpha_2(1-\eta^2)]^{1/2}\ . \tag{15}$$

It is also known that Eq. (14) represents the acoustic branch and Eq. (15) the optical branch for $0<\alpha_1\le 1$ and $0<\alpha_2\le 1$. When $\alpha_1,\alpha_2>1$, Eq. (14) gives the optical branch while Eq. (15) gives the acoustic branch. It is remarked that, for convenience, we have defined Eq. (15) such that it differs from Eq. (52) of I by taking the opposite sign. In other words, the energy in this branch is measured in the negative-energy direction. As is seen in the next section, these SSW's have very important influence on the nature of ISW spectra.

The bulk Green's function for the system consisting of the two uncoupled semi-infinite ferrimagnet can then be written as

$$\underline{G}^{(0)}(m,n)=\begin{cases}\underline{G}^{(1)}(m,n), & m,n\le -1\ ,\\ \underline{G}^{(2)}(m,n), & m,n\ge 0\ ,\\ 0, & \text{otherwise}\ .\end{cases} \tag{16}$$

The supermatrix equation that $G^{(0)}(m,n)$ satisfies is

$$\begin{bmatrix}\vdots & & & & & & \\ \cdots & E\underline{1}-\underline{D}^{(2)} & -\underline{F}^{(2)}_2 & 0 & & & \\ & -\underline{F}^{(2)}_1 & E\underline{1}-\underline{D}^{(2)} & -\underline{F}^{(2)}_2 & & & \\ & 0 & -\underline{F}^{(2)}_1 & E\underline{1}-\underline{D}^{(2)}-\underline{V}^{(2)}_{bb} & 0 & 0 & \\ & & 0 & 0 & E\underline{1}-\underline{D}^{(1)}-\underline{V}^{(1)}_{ba} & -\underline{F}^{(1)}_2 & \\ & & & 0 & -\underline{F}^{(1)}_1 & E\underline{1}-\underline{D}^{(1)} & \cdots\\ & & & & & \vdots & \end{bmatrix}\begin{bmatrix}\vdots\\ \underline{G}^{(0)}(2,n)\\ \underline{G}^{(0)}(1,n)\\ \underline{G}^{(0)}(0,n)\\ \underline{G}^{(0)}(-1,n)\\ \underline{G}^{(0)}(-2,n)\\ \vdots\end{bmatrix}=\begin{bmatrix}\vdots\\ \delta_{2n}\underline{1}\\ \delta_{1n}\underline{1}\\ \delta_{0,n}\underline{1}\\ \delta_{-1n}\underline{1}\\ \delta_{-2n}\underline{1}\\ \vdots\end{bmatrix}\ . \tag{17}$$

Apart from those given in (5) and (6), matrices involved in (17) are defined by

$$\underline{D}^{(i)}=\begin{bmatrix} -8J_i\langle S^z\rangle_b^{(i)} & 4J_i\langle S^z\rangle_a^{(i)}\eta(\kappa) \\ 4J_i\langle S^z\rangle_b^{(i)}\eta(\kappa) & -8J_i\langle S^z\rangle_a^{(i)} \end{bmatrix}, \tag{18}$$

$$F_{\underline{1}}^{(i)}=\begin{bmatrix} 0 & 4J_i\langle S^z\rangle_a^{(i)}\eta(\kappa) \\ 0 & 0 \end{bmatrix}, \tag{19}$$

$$F_{\underline{2}}^{(2)}=\begin{bmatrix} 0 & 0 \\ 4J_i\langle S^z\rangle_b^{(i)}\eta(\kappa) & 0 \end{bmatrix}. \tag{20}$$

When $J_{12}\neq 0$, the two ferrimagnets couple to one another via the nearest-neighbor interactions and the bulk Green's function for the system can be written down from (17) as

$$\begin{bmatrix} & \vdots & & & & & \\ \cdots & E\underline{1}-\underline{D}^{(2)} & -\underline{F}_2^{(2)} & 0 & & & \\ & -\underline{F}_1^{(2)} & E\underline{1}-\underline{D}^{(2)} & -\underline{F}_2^{(2)} & 0 & & \\ & 0 & -\underline{F}_1^{(2)} & E\underline{1}-\underline{D}^{(2)}-\underline{V}_{bb}^{(2)}-\underline{V}_{00} & -\underline{V}_{0,-1} & 0 & \\ & & 0 & \underline{V}_{-1,0} & E\underline{1}-\underline{D}^{(1)}-\underline{V}_{ba}^{(1)}-\underline{V}_{-1,-1} & -\underline{F}_2^{(1)} & \\ & & & 0 & \underline{F}_1^{(1)} & E\underline{1}-\underline{D}^{(1)} & \cdots \\ & & & & & \vdots & \end{bmatrix} \begin{bmatrix} \vdots \\ \underline{G}(2,n) \\ \underline{G}(1,n) \\ \underline{G}(0,n) \\ G(-2,b) \\ G(-2,n) \\ \vdots \end{bmatrix} = \begin{bmatrix} \vdots \\ \delta_{2n}\underline{1} \\ \delta_{1n}\underline{1} \\ \delta_{0n}\underline{1} \\ \delta_{-1n}\underline{1} \\ \delta_{-2n}\underline{1} \\ \vdots \end{bmatrix}, \tag{21}$$

where we have defined the matrices

$$\underline{V}_{00}=\begin{bmatrix} 0 & 0 \\ 0 & -4J_{12}\langle S^z\rangle_a^{(1)} \end{bmatrix}, \qquad \underline{V}_{-1-1}=\begin{bmatrix} -4J_{12}\langle S^z\rangle_b^{(2)} & 0 \\ 0 & 0 \end{bmatrix}, \tag{22}$$

$$\underline{V}_{0-1}=\begin{bmatrix} 0 & 0 \\ 4J_{12}\langle S^z\rangle_b^{(2)}\eta(\kappa) & 0 \end{bmatrix}, \qquad \underline{V}_{-10}=\begin{bmatrix} 0 & 4J_{12}\langle S^z\rangle_a^{(1)}\eta(\kappa) \\ 0 & 0 \end{bmatrix}. \tag{23}$$

It is easily seen from (21) that the diagonal perturbations $\underline{V}_{00}$ and $\underline{V}_{-1-1}$ act only on spins on the surface layers of the two semi-infinite ferrimagnets. They may be regarded as extra effective surface potentials adding to $\underline{V}_{bb}$ and $\underline{V}_{ba}$ in a similar fashion as in Ref. 1. With only the diagonal perturbation due to the interface, the Green's function for the bulk system still satisfies Eqs. (16) and (17) provided that the surface potentials in (5a) and (6a) are replaced by

$$\underline{V}_{ba}^{(1)}=\begin{bmatrix} 4\Delta J_1\langle S^z\rangle_b^{(1)} & 0 \\ 0 & 0 \end{bmatrix}, \tag{24a}$$

$$\underline{V}_{bb}^{(2)}=\begin{bmatrix} 0 & 0 \\ 0 & 4\Delta J_2\langle S^z\rangle_a^{(2)} \end{bmatrix}, \tag{24b}$$

where we have defined

$$\Delta J_1=J_1-J_{12}\alpha_b \tag{25a}$$

$$\Delta J_2=J_2-J_{12}/\alpha_a, \tag{25b}$$

$$\alpha_a=\langle S^z\rangle_a^{(2)}/\langle S^z\rangle_a^{(1)}, \tag{26a}$$

$$\alpha_b=\langle S^z\rangle_b^{(2)}/\langle S^z\rangle_b^{(1)}. \tag{26b}$$

The off-diagonal perturbation $\underline{V}_{0-1}$ and $\underline{V}_{-10}$ come from the coupling between surfaces across the interface. Their contribution can be included by making use of the Dyson equation

$$\underline{G}(m,n)=\underline{G}^{(0)}(m,n)+\sum_{l,l'}\underline{G}^{(0)}(m,l)\underline{V}_{l,l'}\underline{G}(l',n), \tag{27}$$

from which we find the interface Green's function expressed in terms of $G^{(0)}(m,n)$ with the surface potentials (24)

$$\underline{G}(m,n)=\begin{cases} \underline{G}^{(0)}(m,n)+\underline{G}^{(0)}(m,0)\underline{V}_{0-1}\underline{G}(-1,n), & m\geq 0, \\ \underline{G}^{(0)}(m,n)+\underline{G}^{(0)}(m,-1)\underline{V}_{-1,0}G(0,n), & m\leq -1. \end{cases} \tag{28}$$

After some algebra, we obtain the more explicit forms

$$\underline{G}(m,n)=\begin{cases} \underline{G}^{(0)}(m,n)+\underline{G}^{(0)}(m,0)\underline{V}_{0-1}[\underline{1}-\underline{G}^{(0)}(-1,-1)\underline{V}_{-1,0}\underline{G}^{(0)}(0,0)\underline{V}_{0-1}]^{-1} \\ \quad\times[\underline{G}^{(0)}(-1,-1)\underline{V}_{-10}\underline{G}^{(0)}(0,n)+\underline{G}^{(0)}(-1,n)], \quad m\geq 0, \end{cases} \tag{29a}$$

$$\begin{cases} \underline{G}^{(0)}(m,n)+\underline{G}^{(0)}(m,-1)\underline{V}_{-10}[\underline{1}-\underline{G}^{(0)}(0,0)\underline{V}_{0-1}\underline{G}^{(0)}(-1,-1)\underline{V}_{-10}]^{-1} \\ \quad\times[\underline{G}^{(0)}(0,0)\underline{V}_{0-1}\underline{G}^{(0)}(-1,n)+\underline{G}^{(0)}(0,n)], \quad m\leq -1. \end{cases} \tag{29b}$$

For $n=m$, Eqs. (28) can be further simplified with the aid of (16)

$$\underline{G}(m,m)=\begin{cases}\underline{G}^{(2)}(m,m)+\underline{G}^{(2)}(m,0)\underline{V}_{0-1}[\underline{1}-\underline{G}^{(1)}(-1,-1)\underline{V}_{-10}\underline{G}^{(2)}(0,0)\underline{V}_{0-1}]^{-1} \\ \quad\times\underline{G}^{(1)}(-1,-1)\underline{V}_{-10}\underline{G}^{(2)}(0,m), \quad m\geq 0\ , & \text{(30a)} \\ \underline{G}^{(1)}(m,m)+\underline{G}^{(1)}(m,-1)\underline{V}_{-10}[\underline{1}-\underline{G}^{(2)}(0,0)\underline{V}_{0-1}\underline{G}^{(1)}(-1,-1)\underline{V}_{-1,0}]^{-1} \\ \quad\times\underline{G}^{(2)}(0,0)V_{0-1}\underline{G}^{(1)}(-1,m), \quad m\leq -1, & \text{(30b)}\end{cases}$$

where $G^{(1)}(m,n)$ and $G^{(2)}(m,n)$ are given by Eqs. (3) and (4) with the potentials (5a) and (6a) replaced by (24). Equations (29) and (30) express the interface Green's functions in terms of the already known semi-infinite Green's functions.

IV. ISW SPECTRA

The interface spin-wave spectra are determined by the pole of the inverse matrix involved in the second term of Eqs. (30). It is easy to see that the matrices

$$\underline{1}-\underline{G}^{(1)}(-1,-1)\underline{V}_{-10}\underline{G}^{(2)}(0,0)\underline{V}_{0-1}$$

and

$$\underline{1}-\underline{G}^{(2)}(0,0)\underline{V}_{0-1}\underline{G}^{(1)}(-1,-1)\underline{V}_{-10}$$

have the same determinant value. Thus the ISW spectra are uniquely determined by the equation

$$\det|\underline{1}-\underline{G}^{(1)}(-1,-1)\underline{V}_{-10}\underline{G}^{(2)}(0,0)\underline{V}_{0-1}|=0\ . \tag{31}$$

To solve this equation, we start with Eqs. (3) and (4). Using $\underline{V}_{2f}^{(1)}$ and $\underline{V}_{1f}^{(2)}$ in (5) and (6), and V_{ba} and V_{bb} in (24), we find after a long but straightforward calculation,

$$\underline{G}^{(1)}(m,n)=\begin{bmatrix}g_{aa}^{(1)}(m,n)+M_{11}^{(1)}(m)g_{aa}^{(1)}(-1,n) & g_{ab}^{(1)}(m,n)+M_{11}^{(1)}(m)g_{ab}^{(1)}(-1,n) \\ g_{ba}^{(1)}(m,n)+M_{21}^{(1)}(m)g_{aa}^{(1)}(-1,n) & g_{bb}^{(1)}(m,n)+M_{21}^{(1)}(m)g_{ab}^{(1)}(-1,n)\end{bmatrix}, \tag{32}$$

$$\underline{G}^{(2)}(m,n)=\begin{bmatrix}g_{aa}^{(2)}(m,n)+M_{12}^{(2)}(m)g_{ba}^{(2)}(0,n) & g_{ab}^{(2)}(m,n)+M_{12}^{(2)}(m)g_{bb}^{(2)}(0,n) \\ g_{ba}^{(2)}(m,n)+M_{22}^{(2)}(m)g_{ba}^{(2)}(0,n) & g_{bb}^{(2)}(m,n)+M_{22}^{(2)}(m)g_{bb}^{(2)}(0,n)\end{bmatrix}. \tag{33}$$

In these equations we have defined the matrix

$$\begin{aligned}\underline{M}(m)&=\begin{bmatrix}M_{11}^{(1)}(m) & M_{12}^{(2)}(m) \\ M_{21}^{(1)}(m) & M_{22}^{(2)}(m)\end{bmatrix} \\ &=\begin{bmatrix}4\langle S^z\rangle_b^{(1)}[\Delta J_1 g_{aa}^{(1)}(m,-1)-J_1\eta g_{ab}^{(1)}(m,0)]/\Delta^{(1)} & 4\langle S^z\rangle_a^{(2)}[\Delta J_2 g_{ab}^{(2)}(m,0)-J_2\eta g_{aa}^{(2)}(m,-1)]/\Delta^{(2)} \\ 4\langle S^z\rangle_b^{(1)}[\Delta J_1 g_{ba}^{(1)}(m,-1)-J_1\eta g_{bb}^{(1)}(m,0)]/\Delta^{(1)} & 4\langle S^z\rangle_a^{(2)}[\Delta J_2 g_{bb}^{(2)}(m,0)-J_2\eta g_{ba}^{(2)}(m,-1)]/\Delta^{(2)}\end{bmatrix},\end{aligned} \tag{34}$$

where

$$\Delta^{(1)}=1-4\langle S^z\rangle_b^{(1)}[\Delta J_1 g_{aa}^{(1)}(-1,-1)-J_1\eta g_{ab}^{(1)}(-1,0)]\ , \tag{35}$$

$$\Delta^{(2)}=1-4\langle S^z\rangle_a^{(2)}[\Delta J_2 g_{bb}^{(2)}(0,0)-J_2\eta g_{ba}^{(2)}(0,-1)]\ . \tag{36}$$

Combining Eqs. (32)–(36) and plugging the results into (31), we can after a tedious calculation eventually reduce it to the form

$$\Delta^{(1)}\Delta^{(2)}-16J_{12}^2\eta^2\langle s^z\rangle_a^{(1)}\langle S^z\rangle_b^{(2)} \times g_{aa}^{(1)}(-1,-1)g_{bb}^{(2)}(0,0)=0\ , \tag{37}$$

where use has been made of (22) and (23).

We are interested in the ISW's localized in the neighborhood of the interface. As a matter of fact, it is not difficult to see that the last term of Eqs. (30) decreases exponentially with increasing $|m|$, provided that the energy of the system falls outside the bulk energy band of either medium 1 or 2. In other words, when $T_i^2>1$, the interface part of the Green's function decays exponentially when it moves away from the interface. Substituting (35) and (36) into (37), we find under the conditions $T_i^2>1$

$$\begin{aligned}&(\varepsilon_1+1)(\varepsilon_2-\alpha_2)(\eta^2-1)J_{12}^2 \\ &\quad+\left[\frac{1}{\alpha_b}\Delta_1(\varepsilon_2-\alpha_2)-\alpha_a\Delta_2(\varepsilon_1+1)\right]J_{12} \\ &\quad+\frac{\alpha_1}{\alpha_2}\Delta_1\Delta_2=0\ ,\end{aligned} \tag{38}$$

where

$$\Delta_1=J_1(\varepsilon_1+1) -\tfrac{1}{2}J_1\eta^2[-T_1+1-\mathrm{sgn}(T_1)(T_1^2-1)^{1/2}] , \quad (39)$$

$$\Delta_2=-J_2(\varepsilon_2-\alpha_2) -\tfrac{1}{2}J_2\alpha_2\eta^2[-T_2+1-\mathrm{sgn}(T_2)(T_2^2-1)^{1/2}] . \quad (40)$$

It is noted that Eqs. (39) and (40) yield the surface spin-wave spectra for the semi-infinite ferrimagnets when $\Delta_1=0$ and $\Delta_2=0$. The corresponding solutions are given by (14) and (15).

We have derived the ISW spectrum equations for the *a-b* antiferromagnetic interface as in Fig. 1(a). It is a simple matter to find the ISW spectra for the *a-a* or *b-b* ferromagnetic interface from the above result. Since these latter interfaces are completely symmetric with respect to the interchange of *a* and *b* sublattices, we have to consider only one of them.

The *a-a* ferromagnetic coupling is obtained from the above by interchanging the *a* and *b* sublattices in one of the semi-infinite ferrimagnets of a system as shown in Fig. 1(a), and at the same time replacing the antiferromagnetic exchange integral $J_{12}>0$ by the ferromagnetic $J_{12}<0$ across the interface. This procedure does not change the form of the Hamiltonian (1). The equation of the *a-a* ferromagnetic ISW spectrum then follows from (38) by making the interchange in the medium 2,

$$\langle S^z\rangle_a^{(2)}\rightleftarrows\langle S^z\rangle_b^{(2)} . \quad (41)$$

This transformation is completely equivalent to the following replacements in Eq. (38):

$$\alpha_2\rightarrow 1/\alpha_2 , \quad \varepsilon_2\rightarrow -\varepsilon_2/\alpha_2 , \quad \alpha_a\rightarrow -\alpha_2\alpha_a , \quad \alpha_b\rightarrow -\alpha_b/\alpha_2 . \quad (42)$$

The meaning of all the parameters remains the same after either the transformation (41) or (42). The resulting equation for the ISW spectrum for an *a-a* ferromagnetic coupling across the interface is then

$$(\varepsilon_1+1)(\varepsilon_2+1)(\eta^2-1)J_{12}^2 - \left[\frac{\alpha_2}{\alpha_b}\Delta_1(\varepsilon_2+1)+\alpha_2\alpha_a\Delta_2(\varepsilon_1+1)\right]J_{12} -\alpha_1\alpha_2\Delta_1\Delta_2=0 . \quad (43)$$

where Δ_1 is still given by (39) while Δ_2 is given by

$$\Delta_2=J_2(\varepsilon_2+1) -\tfrac{1}{2}J_2\eta^2[-T_2+1-\mathrm{sgn}(T_2)(T_2^2-1)^{1/2}] \quad (44)$$

instead of (40). Once more, $\Delta_1=0$ and $\Delta_2=0$ represents surface spin waves in medium 1 and medium 2, respectively. Since Eq. (44) has the same form as (39) but not (40), the situation is different from the *a-b* antiferromagnetic case. Medium 2 contributes an acoustic surface branch when $0<\alpha_2\leq 1$, but an optical surface branch when $\alpha_2>1$. Furthermore, these surface branches appear in the positive-energy direction.

We now turn our attention to the type of interface coupling scheme as depicted in Fig. 1(b). For the *a-b* antiferromagnetic interface the only difference from the previous case shown in Fig. 1(a) is the coupling potential across the interface. Matrices (22) and (23) should be replaced by

$$\underline{V}_{00}=\begin{bmatrix}0 & 0\\ 0 & -J_{12}\langle S^z\rangle_a^{(1)}\end{bmatrix}, \quad \underline{V}_{-1,-1}=\begin{bmatrix}-J_{12}\langle S^z\rangle_b^{(2)} & 0\\ 0 & 0\end{bmatrix}, \quad (45)$$

$$\underline{V}_{0-1}=\begin{bmatrix}0 & 0\\ J_{12}\langle S^z\rangle_b^{(2)} & 0\end{bmatrix}, \quad \underline{V}_{-1,0}=\begin{bmatrix}0 & J_{12}\langle S^z\rangle_a^{(1)}\\ 0 & 0\end{bmatrix} . \quad (46)$$

This can be understood as follows. In Fig. 1(a) each ion on the surface of one medium is coupled to four nearest neighbors across the interface, while in Fig. 1(b) each ion has only one nearest neighbor across the interface. Furthermore, the η factor is missing in the off-diagonal matrix elements because the line connecting the ions coupled across the interface in Fig. 1(b) is normal to the interface. Thus the spectrum equation can be obtained by following exactly the same procedures as before and the result is

$$\left[\frac{1}{\alpha_b}\Delta_1(\varepsilon_2-\alpha_2)-\alpha_a\Delta_2(\varepsilon_1+1)\right]J_{12}+\frac{\alpha_1}{\alpha_2}\Delta_1\Delta_2=0, \quad (47)$$

where both Δ_1 and Δ_2 remain the same and are still given by (39) and (40). When the transformation (42) is made in (47), we obtain directly the spectrum equation for the *a-a* ferromagnetic interface

$$\left[\frac{\alpha_2}{\alpha_b}\Delta_1(\varepsilon_2+1)+\alpha_a\alpha_2\Delta_2(\varepsilon_1+1)\right]J_{12}+\alpha_1\alpha_2\Delta_1\Delta_2=0 , \quad (48)$$

where Δ_2 is still given by (44).

From the above discussion, we find that the ISW spectra for different types of interface coupling can be qualitatively different. The ISW spectra (47) and (48) for the interface as in Fig. 1(b) involve only linear terms in J_{12}, while (38) and (43) for the interface as in Fig. 1(a) have J_{12}^2 terms as well. Without going into the detailed analysis, we just mention that the difference is originated by the different orientation of the line joining the coupled nearest-neighbor spins across the interface. As is shown in the Appendix, however, all the four spectrum equations have the same asymptotic behavior. As the interface coupling diminishes, or when $J_{12}\rightarrow 0$, two of the interface spin waves in each case reduce to SSW's of the two semi-infinite media. Similar result is found in a one-dimensional antiferromagnetic chain with an impurity bond,[13] except that the two localized modes are degenerate.

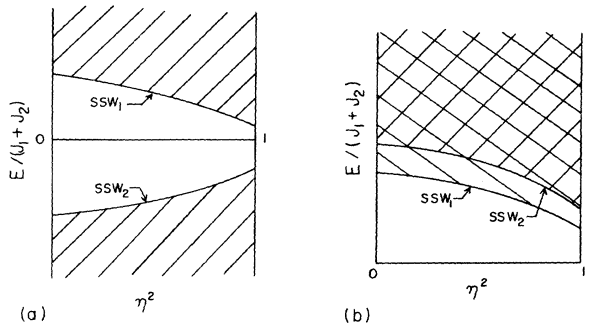

FIG. 2. Schematic diagram illustrates the energy region (shaded area) where ISW can occur. Thus, ISW_1 may be found in the region between SSW_1 and SSW_2. The SSW's serve as lower bounds of the ISW's in each medium. The SSW's can be either acoustic or optical depending on the parameters α_1 and α_2. (a) *a-b* antiferromagnetic interface coupling, and (b) *a-a* ferromagnetic interface coupling.

As is shown in the Appendix, the ISW's always appear outside the energy region of the SSW's. For positive energies, ISW's are above the SSW energy spectrum and for negative energies, ISW's are below the SSW spectrum. In other words, the two surface waves serve as the lower bounds of the ISW spectrum. The situation is illustrated for certain range of the parameters α_1 and α_2 in Fig. 2 in which the energy region where solutions to the ISW spectrum equations (38) and (43) can possibly exist is shown by the shaded area. For example, only ISW_1 may be found in the region between SSW_1 and SSW_2 in Fig. 2(b), while both ISW's can exist in the shaded area. In any case, however, the ISW's are always outside the bulk spin-wave spectra, which are also in the shaded area and are not shown in the figure. It will be observed in the following that the ISW's move toward large $|E|$ values as $|J_{12}|$ increases. We remark at this point that the ISW solution discussed here is stable because we are considering only a specific interface configuration. In general one has to study the complicated energy relations with interface magnetic structures. This will be discussed in our future investigations.

V. RESULTS AND DISCUSSION

We present in this section numerical results of the ISW spectra for different cases. For convenience, we have taken J_1+J_2 to be the unit of energy.

Spin parameters are chosen from Table II of Ref. 12 in our calculation. For the interface contact type as illustrated in Fig. 1(a), the ISW spectra for various interface coupling schemes are plotted in Figs. 3–8. For the antiferromagnetic-antiferromagnet interface with *a-b* antiferromagnetic coupling for which $\langle S^z\rangle_a^{(i)}=\langle S^z\rangle_b^{(i)}$, $i=1,2$, the ISW spectra are given in Fig. 3 and the spectra for the antiferromagnet/ferromagnet for which $\langle S^z\rangle_a^{(1)}=-\langle S^z\rangle_b^{(1)}$ but $\langle S^z\rangle_a^{(2)}\neq-\langle S^z\rangle_b^{(2)}$ with antiferromagnetic coupling are shown in Fig. 4. In Figs. 5–7

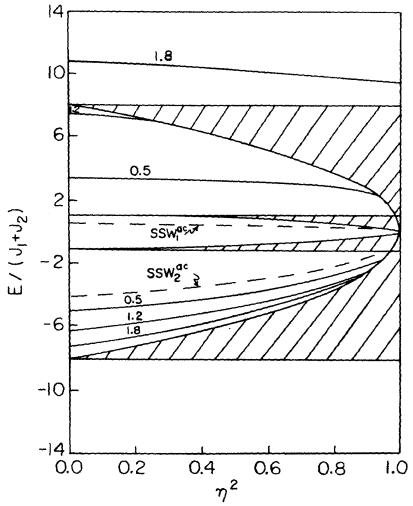

FIG. 3. *a-b* antiferromagnetic ISW spectra in an antiferromagnet/ferromagnet system as in Fig. 1(a). $S_a^{(1)}=0.5$, $S_a^{(2)}=1.5$, $\langle S^z\rangle_a^{(1)}=0.447$, $\langle S^z\rangle_a^{(2)}=1.441$, $\alpha_1=\alpha_2=1$, and $J_1=0.3$. Solid lines represent the ISW's with corresponding J_{12} values marked. Dashed lines are the SSW's ($J_{12}=0$) and the shaded areas are the bulk spectra.

we plot the spectra for the ferrimagnet/ferrimagnet interface with *a-b* antiferromagnetic coupling for α_1 and α_2 in different ranges of choice. The ferrimagnet/ferrimagnet interface with *a-a* ferromagnetic coupling is given in Fig. 8.

For interface contacts of the type as in Fig. 1(b), we calculate ISW spectra for ferrimagnet/ferrimagnet interface with *a-b* antiferromagnetic and *a-a* ferromagnetic couplings. The results are shown in Figs. 9 and 10, re-

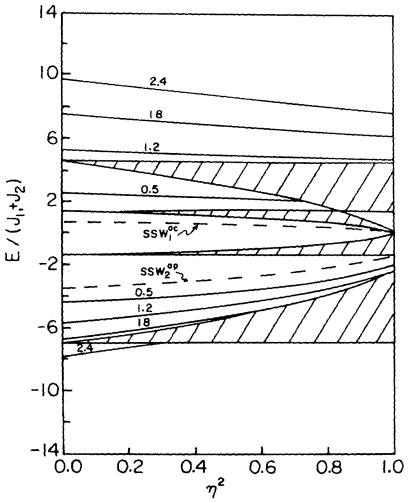

FIG. 4. Same as in Fig. 3 for an antiferromagnet-ferromagnet system with parameters $S_a^{(1)}=0.5$, $S_a^{(2)}=1.5$, $\langle S^z\rangle_a^{(1)}=0.447$, $\langle S^z\rangle_a^{(2)}=1.449$, $\alpha_1=1$, $\alpha_2=0.655$, and $J_1=0.4$.

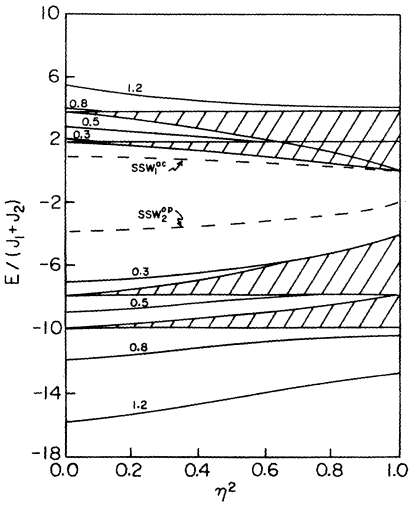

FIG. 5. Same as in Fig. 3 for a ferrimagnet-ferrimagnet system with parameters $S_a^{(1)}=2.5$, $S_a^{(2)}=2$, $\langle S^z\rangle_a^{(1)}=2.479$, $\langle S^z\rangle_a^{(2)}=1.957$, $\alpha_1=0.194$, $\alpha_2=0.489$, and $J_1=0.5$. The SSW is acoustic in medium 1 and optical in medium 2 in this case.

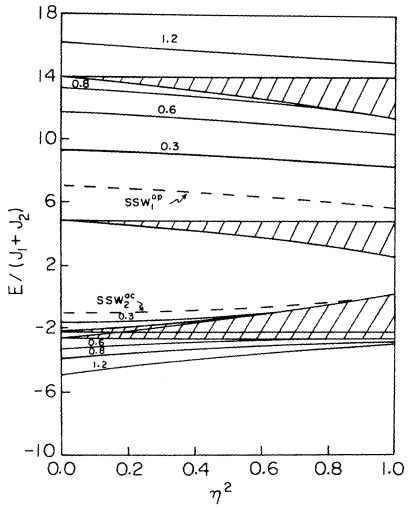

FIG. 7. Same as in Fig. 5 except for the parameters $S_a^{(1)}=0.5$, $S_a^{(2)}=2$, $\langle S^z\rangle_a^{(1)}=0.481$, $\langle S^z\rangle_a^{(2)}=0.957$, $\alpha_1=5.155$, $\alpha_2=2.045$, and $J_1=0.7$. The SSW is optical in medium 1 and acoustic in medium 2 in this case.

spectively. For easier comparison, the corresponding bulk as well as SSW spectra for each medium are also plotted in all cases.

There are qualitative features common to all cases we have calculated. First of all, we observe that ISW spectra fall outside the energy range of the corresponding SSW's. When J_{12} decreases and approaches zero, as has been pointed out above, there are indeed two ISW's tending to SSW's on each surface separately. For arbitrary J_{12}, we find that there are two and only two ISW's localized on the interface. Since these two modes of ISW's become the corresponding surface waves when the two semi-infinite systems are decoupled, we conclude that these ISW's are localized on the two sides of the interface. For the *a-b* antiferromagnetic interface as in Fig. 1(a), these waves are localized on the *a* sublattice in medium 1 and on the *b* sublattice in medium 2. Similarly, the ISW's will be localized on the *a* sublattices on both sides of the *a-a* ferromagnetic interface. It is easily verified that the α

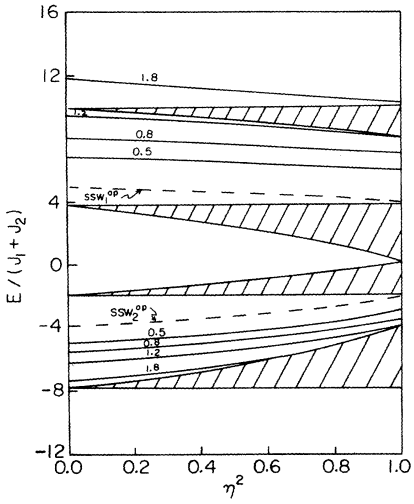

FIG. 6. Same as in Fig. 5 except for the parameters $S_a^{(1)}=0.5$, $S_a^{(2)}=2$, $\langle S^z\rangle_a^{(1)}=0.481$, $\langle S^z\rangle_a^{(2)}=1.957$, $\alpha_1=5.155$, $\alpha_2=0.489$, and $J_1=0.5$. Both SSW's are optical in this case.

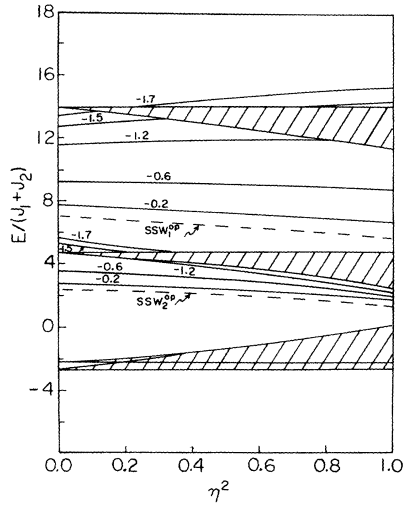

FIG. 8. *a-a* ferromagnetic ISW spectra in a ferrimagnet-ferrimagnet system as in Fig. 1(a). $S_a^{(1)}=0.5$, $S_a^{(2)}=1$, $\langle S^z\rangle_a^{(1)}=0.481$, $\langle S^z\rangle_a^{(2)}=0.957$, $\alpha_1=5.155$, $\alpha_2=2.045$, and $J_1=0.7$.

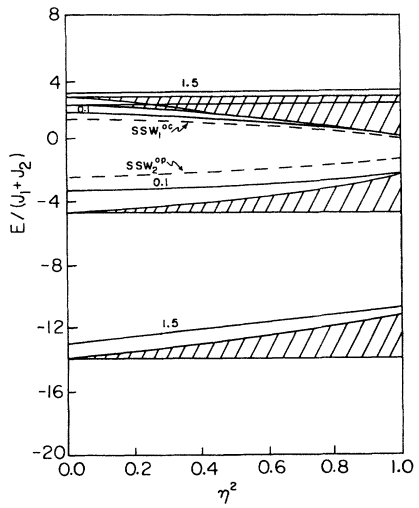

FIG. 9. *a-b* antiferromagnetic ISW spectra in a ferrimagnet/ferrimagnet system as in Fig. 1(b). $S_a^{(1)}=2.5$, $S_a^{(2)}=2$, $\langle S^z\rangle_a^{(1)}=2.479$, $\langle S^z\rangle_a^{(2)}=1.957$, $\alpha_1=0.194$, $\alpha_2=0.489$, and $J_1=0.7$.

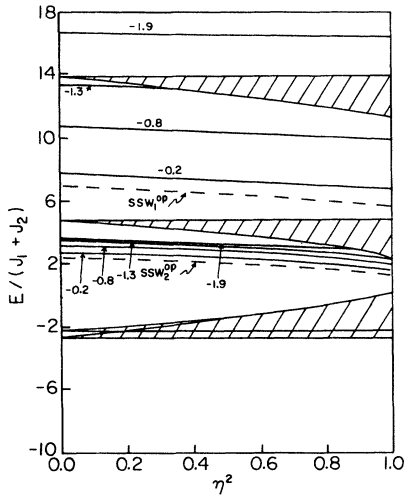

FIG. 10. *a-b* antiferromagnetic ISW spectra in a ferrimagnet/ferrimagnet system as in Fig. 1(b). $S_a^{(1)}=0.5$, $S_a^{(2)}=1$, $\langle S^z\rangle_a^{(1)}=0.481$, $\langle S^z\rangle_a^{(2)}=0.957$, $\alpha_1=5.155$, $\alpha_2=2.045$, and $J_1=0.7$.

and β states localized on both sides of the interface in Ref. 8 are just special cases and can be reproduced by setting $S_a^{(1)}$, $S_b^{(1)}$, $S_a^{(2)}$, and $S_b^{(2)}$ all equal to unity.

APPENDIX

We now study the asymptotic behavior of the ISW's as $J_{12}\to 0$, and show that they actually tend to the SSW's from the larger absolute-energy value. Since the procedures are the same for all four spectrum equations (38), (43), (47), and (48), we consider only (38) in the following.

Solving for J_{12}, we have, from (38),

$$J_{12}=\frac{-(\Gamma\varepsilon_1-\alpha_2)\Delta_1/\alpha_b+(\varepsilon_1+1)\Delta_2\alpha_a\pm\sqrt{\Delta}}{2(\varepsilon_1+1)(\Gamma\varepsilon_1-\alpha_2)(\eta^2-1)}\ , \tag{A1}$$

where we have defined

$$\Delta=[(\Gamma\varepsilon_1-\alpha_2)\Delta_1/\alpha_b-(\varepsilon_1+1)\Delta_2\alpha_a]^2 -4(\varepsilon_1+1)(\Gamma\varepsilon_1-\alpha_2)(\eta^2-1)\Delta_1\Delta_2\alpha_a/\alpha_b\ , \tag{A2}$$

$$\Gamma=J_1\langle S_z\rangle_a^{(1)}/J_2\langle S^z\rangle_a^{(2)}=\varepsilon_2/\varepsilon_1\ . \tag{A3}$$

In (A2) and (A3), we have made use of the relation

$$\alpha_a/\alpha_b=\alpha_1/\alpha_2\ , \tag{A4}$$

and Δ_1,Δ_2 are given by (39) and (40), respectively.

We first look at the analytic behavior of (A1) near $\varepsilon_1^{\rm SSW}$. Let

$$\varepsilon_1=\varepsilon_1^{\rm SSW}+\Delta\varepsilon_1\ , \tag{A5}$$

in which $\Delta\varepsilon_1$ is a small quantity. Since $\Delta_1(\varepsilon_1^{\rm SSW})=0$, we expand $\Delta_1(\varepsilon_1)$ and keep terms of the order of $\Delta\varepsilon_1$; that is,

$$\Delta_1=\{J_1+\tfrac{1}{2}J_1\eta^2[1+\tfrac{1}{2}\,\mathrm{sgn}(T_1)T_1(T_1^2-1)^{-1/2}]T_i'\}\Delta\varepsilon_1\ , \tag{A6}$$

$$T_1=1+(\varepsilon_1^{\rm SSW}+1)(\varepsilon_1^{\rm SSW}-\alpha_1)(\alpha_1\eta^2/2)^{-1}\ , \tag{A7}$$

$$T_1'=(2\varepsilon_1^{\rm SSW}+1-\alpha_1)(\alpha_1\eta^2/2)^{-1}\ . \tag{A8}$$

Similarly, we expand $\sqrt{\Delta}$ to the first order in Δ_1:

$$\sqrt{\Delta}\approx|(\varepsilon_1+1)\Delta_2\alpha_a| -\mathrm{sgn}[\Delta_2\alpha_a(\varepsilon_1^{\rm SSW}+1)]\frac{2\Delta_1}{\alpha_b}(\eta^2-\tfrac{1}{2})(\Gamma\varepsilon_1^{\rm SSW}-\alpha_2)\ . \tag{A9}$$

Substituting (A9) in (A1), we find an approximate expression for J_{12} to the first order in Δ_1 and $\Delta\varepsilon_1$, from which a solution $J_{12}\to 0+$ as $\Delta\varepsilon_1\to 0$ can be identified, namely,

$$J_{12}\approx\Delta_1/\alpha_b(\varepsilon_1^{\rm SSW}+1)\ , \tag{A10}$$

where Δ_1 is given by (A6). In other words, we have shown that the ISW approaches a SSW because $\varepsilon_1\to\varepsilon_1^{\rm SSW}$ as $J_{12}\to 0$. Evidently, the sign of J_{12} is determined by that of $\Delta\varepsilon_1$ because $\mathrm{sgn}(T_1)T_1\geq 0$, $J_1\geq 0$, and $T_1'\geq 0$ can be seen from (14). Therefore, only when $\Delta\varepsilon_1\to 0+$, $J_{12}\to 0+$, or $\varepsilon_1=\varepsilon_1^{\rm SSW}+\Delta\varepsilon_1>\varepsilon_1^{\rm SSW}$.

Next, we look at the behavior of (A1) near $\varepsilon_2^{\rm SSW}$. For an arbitrary small quantity $\Delta\varepsilon_2=\varepsilon_2-\varepsilon_2^{\rm SSW}$, we can now expand $\Delta_2(\varepsilon_2)$ to the first order in $\Delta\varepsilon_2$

$$\Delta_2=\{-J_2+\tfrac{1}{2}\alpha_2J_2\eta^2 \times[1+\tfrac{1}{2}\,\mathrm{sgn}(T_2)(T_2-1)^{-1/2}T_2]T_2'\}\Delta\varepsilon_2\ , \tag{A11}$$

$$T_2=1+(\varepsilon_2^{\rm SSW}+1)(\varepsilon_2^{\rm SSW}-\alpha_2)[(\alpha_2/2)\eta^2]^{-1}\ , \tag{A12}$$

$$T_2'=(2\varepsilon_2^{\rm SSW}+1-\alpha_2)[(\alpha_2/2)\eta^2]^{-1}\ , \tag{A13}$$

where we have made use of the fact that $\Delta_2(\varepsilon_2^{\rm SSW})=0$. The exchange coupling J_{12} is now a function of ε_2 and can be expanded to the first order in Δ_2 and $\Delta\varepsilon_2$. In a similar fashion, we find the solution

$$J_{12}=\alpha_a\Delta_2/(\alpha_2-\varepsilon_2^{\mathrm{SSW}}) , \tag{A14}$$

which approaches zero as $\Delta\varepsilon_2\to 0$. Since α_2 and α_a are both positive, but $\varepsilon_2^{\mathrm{SSW}}$ is always negative, as is clearly seen from (15), we conclude that J_{12} and Δ_2 have the same sign. On the other hand, $J_2>0$, $\mathrm{sgn}(T_2)T_2\geq 0$ and $T_2'<0$, we see that J_{12} and $\Delta\varepsilon_2$ have opposite signs. This means that $J_{12}\to 0+$ as $\Delta\varepsilon_2\to 0$. Therefore, the energy of the ISW in medium 2 is below that of the SSW, and tends to $\varepsilon_2^{\mathrm{SSW}}$ from below as $J_{12}\to 0+$.

Following exactly the same procedure, one can show that all the other SSW's have the same behavior and tend to the corresponding SSW's in the limit of the interface decoupling. They are not reproduced here.

[1]A. Yaniv, Phys. Rev. B **28**, 402 (1983).
[2]B. X. Xu, M. Mostoller, and A. K. Rajagopal, Phys. Rev. B **31**, 7431 (1985).
[3]F. Herman, P. Lambia, and O. Jepsen, Phys. Rev. B **31**, 4394 (1985).
[4]L. L. Hinchey and D. L. Mills, Phys. Rev. B **33**, 3329 (1986).
[5]Diep-The-Hung, Phys. Rev. B **40**, 4818 (1989); J. Appl. Phys. **67**, 5667 (1990).
[6]K. Mika and P. Grunberg, Phys. Rev. B **31**, 4465 (1985).
[7]L. Dobrzynski, B. Djafari-Rouhani, and H. Puszkarski, Phys. Rev. B **33**, 3251 (1986).
[8]G. J. Mata and E. Pestana, Phys. Rev. B **42**, 885 (1990).
[9]Diep-The-Hung, L. Harada, and O. Nagai, Phys. Lett. **53A**, 157 (1975).
[10]Diep-The-Hung, Phys. Status Solidi B **82**, 383 (1977).
[11]H. Zeng and D. L. Lin, Phys. Rev. B **37**, 9615 (1988). This paper will be referred to as I.
[12]D. L. Lin and H. Zheng, Phys. Rev. B **37**, 5394 (1988).
[13]G. J. Mata and E. Pestana, Phys. Rev. B **31**, 7285 (1985).